Title

Raman Scattering in Molecular Junctions: A Pseudoparticle Formulation

Journal

Nano Letters, 14(2)

ISSN

1530-6984

Authors

White, Alexander J
Tretiak, Sergei
Galperin, Michael

Publication Date

2014-02-12

DOI

10.1021/nl4039532

Peer reviewed

Raman Scattering in Molecular Junctions: A Pseudoparticle Formulation

Alexander J. White,[†] Sergei Tretiak,[‡] and Michael Galperin[*,†]

Department of Chemistry & Biochemistry, University of California San Diego, La Jolla, CA 92093, USA, and Theoretical Division, Center for Nonlinear Studies (CNLS), and Center for Integrated Nanotechnologies (CINT), Los Alamos National Laboratory, Los Alamos, NM 87545, USA

E-mail: migalperin@ucsd.edu

Abstract

We present a formulation of Raman spectroscopy in molecular junctions, based on a many-body state representation of the molecule. The approach goes beyond the previous effective single orbital formalism, and provides a convenient way to incorporate computational methods and tools proven for equilibrium molecular spectroscopy into the realm of current carrying junctions. The presented framework is illustrated by first principle simulations of Raman response in a three-ring oligophenylene vinylene terminating in amine functional groups (OPV3) junction. The calculated shift in Stokes lines and estimate of vibrational heating by electric current agree with available experimental data. In particular our results suggest that participation of the OPV3 cation in Raman scattering under bias may be responsible for the observed shift, and that the direction of the shift depends on renormalization of normal modes. This work is a step towards atomistic quantum *ab initio* modeling of the optical response of non-equilibrium electronic dynamics in molecular junctions.

Keywords: Raman scattering, molecular junctions, pseudoparticle non-equilibrium Green functions, time-dependent density functional theory (TDDFT), oligophenylene-vinylene (OPV), vibrational heating

[*]To whom correspondence should be addressed

[†]Department of Chemistry & Biochemistry, University of California San Diego, La Jolla, CA 92093, USA

[‡]Theoretical Division, Center for Nonlinear Studies (CNLS), and Center for Integrated Nanotechnologies (CINT), Los Alamos National Laboratory, Los Alamos, NM 87545, USA

Molecular electronics promises to harness electronic functionality over an area of no more than a few molecules thus approaching the fundamental size limit of molecular electronic devices.[1] Our progress in this field is subject to the availability of advanced fabrication technologies and experimental capabilities to precisely characterize the structure and monitor the underlying fundamental electronic dynamics. The first observation of Raman spectroscopy enhancement for molecules chemisorbed on metal surfaces (SERS),[2,3] has manifested an important optical tool for single molecule detection.[4,5] Since then the field has progressed rapidly.[6–9] SERS is known to be dominated by *hot spots* (areas of particularly strong electromagnetic field enhancement).[10] The ability to produce nanometer scale gaps in metal junctions[11–13] paved the way for the application of SERS in molecular electronics as diagnostic and control tool.[14–16] In particular, Raman spectroscopy was used to estimate bias induced vibrational and electronic heating in molecular junctions,[17–19] to reveal the structure of single-molecule junctions,[20–23] and to estimate orientation of a molecule in junction.[24,25] Correlations between the Raman signal and conductance, due to junction dynamics, suggest the possibility to characterize electronic dynamics by optical

means.[18,26,27]

Experimental advances have driven theoretical interest in this field. Several theoretical approaches have been put forward to analyze and explain existing data as well as to propose future experiments.[15,28] In particular, in our previous publications we combined a non-equilibrium Green's function description of quantum transport with a generalized scattering theory of the Raman flux, thus providing the first theoretical description of Raman scattering in such systems. Within simple models we applied the theory to study bias induced vibrational[29,30] and electronic[31,32] heating, charge transfer contribution to SERS,[33] and time-dependent correlations between conductance and Stokes signal.[26,34–36]

To this point existing studies of Raman scattering under non-equilibrium electronic conditions have utilized a noninteracting orbital-based approach (a single-electron mean-field picture), which becomes inadequate in the presence of strong interactions (e.g. molecule-plasmon coupling) in the system.[37] On the other hand only *ab inito* simulations based on equilibrium theory of Raman scattering, were reported in the literature for molecules adsorbed on metal surfaces[21,38–44] and in junctions.[45–47] This necessitates the need for theoretical techniques enabling modeling of optical response of non-equilibrium electronic system in molecular junctions using advanced quantum-chemical methods able to describe the underlying many-body physics.

Here we present a pseudo-particle non-equilibrium Green function (PP-NEGF) formulation for Raman scattering probes in current carrying molecular junctions, and apply it to first principle simulations of Raman scattering in an OPV3 junction (see Fig. 1). This molecular system has been used in Raman spectroscopy experiments.[19] The study is the first attempt of *ab initio* simulation within a non-equilibrium theory of Raman scattering. Our eventual goal is a realistic description of optical response in junctions, where the PP-NEGF molecular Raman scattering (presented here) should be accompanied by PP-NEGF description of interactions with plasmon excitations in the contacts (as presented in Ref.[37]).

We stress that the PP-NEGF approach (relying on the many-body states) introduced here is fundamentally different from the quasiparticle considerations (operating with single-particle orbitals) described in our previous publications.[26,29–36] Particularly, due to the many-body states representation, the PP-NEGF formulation allows one to account for all intra-molecular interactions exactly. It also provides a possibility of a convenient map to the language of vibronic (dressed) states. Note that while the standard (Redfield) quantum master equation in principle can also account exactly for the intra-molecular interactions, it is applicable only to the unphysically high temperature regime ($k_BT \gg \Gamma$)[48] and in the absence of degeneracies in the system.[49] It also completely misses the hybrydization between the molecule and the contacts,[50] which frequently results in qualitative failures.[51] Thereby, the PP-NEGF approach to the Raman scattering is an important theoretical advance, since it provides a convenient way to incorporate tools of quantum chemistry and equilibrium molecular spectroscopy (traditionally formulated in the language of many-body states of an isolated molecule) into the realm of current carrying junctions.[52]

We consider a molecule, M, bridging two metal electrodes, and subjected to an external laser radiation, *rad*. The electrodes act as electronic, L

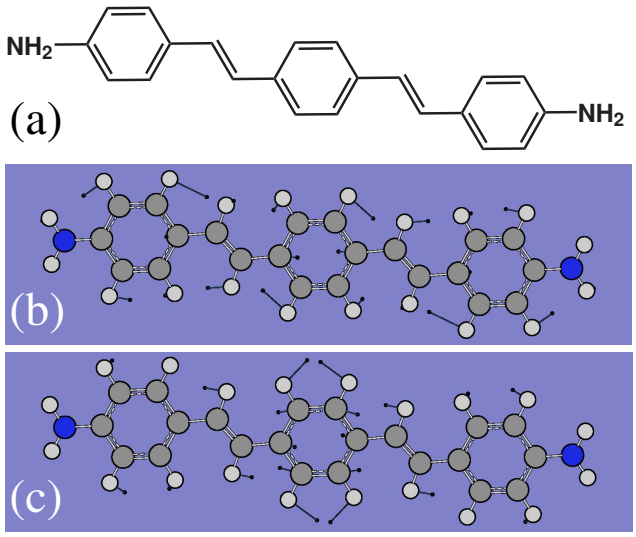

Figure 1: A three-ring oligophenylene vinylene terminating in amine functional groups (OPV3) molecule. Shown are (a) molecular structure and normal modes of neutral OPV3 at frequencies (b) 1199 cm^{-1} and (c) 1608 cm^{-1}. Created by GaussView 5.

and R, and thermal, B, reservoirs, each at its own equilibrium. The Hamiltonian of the junction is

$$\hat{H} = \hat{H}_M + \sum_{K=L,R,B,rad} \left(\hat{H}_K + \hat{V}_K\right) \tag{1}$$

Here we represent the molecular Hamiltonian $\hat{H}_M$ in terms of many-body states $|S\rangle$ of the molecule

$$\hat{H}_M = \sum_{S_1,S_2\in M} H^{(M)}_{S_1S_2} \hat{X}_{S_1S_2} \tag{2}$$

while the Hamiltonians of the baths are expressed within second quantization

$$\begin{aligned} \hat{H}_{L(R)} = \sum_{k\in L(R)} \varepsilon_k \hat{c}^\dagger_k \hat{c}_k, \quad \hat{H}_B = \sum_{\beta\in B} \omega_\beta \hat{b}^\dagger_\beta \hat{b}_\beta, \\ \hat{H}_{rad} = \sum_\alpha \nu_\alpha \hat{a}^\dagger_\alpha \hat{a}_\alpha, \end{aligned} \tag{3}$$

where $\hat{X}_{S_1S_2} \equiv |S_1\rangle\langle S_2|$ is a Hubbard (projection) operator, and $\hat{c}^\dagger_k$ ($\hat{c}_k$), $\hat{b}^\dagger_\beta$ ($\hat{b}_\beta$), and $\hat{a}^\dagger_\alpha$ ($\hat{a}_\alpha$) create (annihilate) an electron in the contacts L and R, phonon in the thermal bath B, and photon of radiation field *rad*, respectively. Finally, $\hat{V}_{L(R)}$, $\hat{V}_B$, and $\hat{V}_{rad}$ in Eq.(1) describe single electron, phonon, and photon transitions between the molecule and baths

$$\hat{V}_K = \sum_{\substack{S_1,S_2\in M \\ q\in K}} \left(V^{(K)}_{S_1S_2,q} \hat{X}^\dagger_{S_1S_2} \hat{O}_q + H.c.\right) \tag{4}$$

Here $\hat{O}_q = \hat{c}_k$, $\hat{b}_\beta$, and $\hat{a}_\alpha$ for $K = L(R)$, B, and *rad*, respectively. Below we utilize molecular vibronic states $|S_m\rangle = |e_m, v^{(m)}_\nu\rangle \approx |e_m\rangle\,|v^{(m)}_\nu\rangle$ as many-body basis, so that $H^{(M)}_{S_1S_2} = \delta_{S_1,S_2} E_{S_1}$, $V^{(L(R))}_{S_1S_2,k} = V_{e_1e_2,k}\,\langle v^{(1)}_{\nu_1}|v^{(2)}_{\nu_2}\rangle$, $V^{(B)}_{S_1S_2,\beta} = \delta_{e_1,e_2} W_{v^{(1)}_1 v^{(1)}_2,\beta}$, and $V^{(rad)}_{S_1S_2,\alpha} = -\vec{\mu}_{e_1,e_2}\vec{\mathscr{E}}_\alpha\,\langle v^{(1)}_{\nu_1}|v^{(2)}_{\nu_2}\rangle$. Here $\vec{\mu}_{e_1,e_2}$ is the electronic transition dipole moment, $\vec{\mathscr{E}}_\alpha$ is amplitude of the radiation field mode α, and $\langle v^{(1)}_{\nu_1}|v^{(2)}_{\nu_2}\rangle$ are overlap integrals of the vibrational wave functions for electronic ($L(R)$) and optical (*rad*) transitions. Corresponding Franck-Condon factors are evaluated following the method by Ruhoff and Ratner.[53,54]

An expression for Raman scattering in current-carrying junctions was first derived considering an outgoing photon flux caused by a coherent photon scattering from an occupied initial, $\alpha = i$, to an empty final, $\alpha = f$, mode of radiation field.[30] The derivation was performed using a noninteracting orbital-based representation. Here we develop a desirable generalization to the many-body molecular basis $\{|S\rangle\}$ by invoking the PP-NEGF method.[55–58] Within this approach one can introduce pseudoparticle operator, $\hat{d}^\dagger_S$, that creates the molecular many-body state $|S\rangle$ by acting on vacuum state, $|S\rangle = \hat{d}^\dagger_S|0\rangle$. The methodology is identical to the second quantization. However, it is formulated in an extended Hilbert space, whose physically relevant subspace is defined by a normalization condition $\sum_S \hat{d}^\dagger_S \hat{d}_S = 1$. In the extended Hilbert space the non-equilibrium pseudo-particle Green function

$$G_{S_1S_2}(\tau_1,\tau_2) = -i\langle T_c\, \hat{d}_{S_1}(\tau_1)\, \hat{d}^\dagger_{S_2}(\tau_2)\rangle \tag{5}$$

satisfies the usual Dyson equation. Restricting the latter to the physical subspace results in a coupled system of equations for projections of the Green function (see e.g. Ref.[57] for details).

Following the line of argument of Ref.[30] and assuming no charge transfer (CT) contribution, an expression for intra-molecular Raman flux which starts in a ground molecular state $|g\rangle$ and proceeds via set of excited states $\{|x\rangle\}$, is given by[59] (see Supporting information for derivation details)

$$\begin{aligned} J(t) = 2\mathrm{Re} \sum_{\substack{g_i,x_1,x_2,g_f \\ \bar{g}_i,\bar{x}_1,\bar{x}_2,\bar{g}_f}} \zeta_{g_i} \int_{-\infty}^{t} dt' \int_{-\infty}^{t} dt_1 \int_{-\infty}^{t'} dt_2 \\ \Pi^<_{g_ix_1,\bar{g}_i\bar{x}_1}(t_1-t_2)\,\Pi^>_{g_fx_2,\bar{g}_f\bar{x}_2}(t'-t) \\ G^>_{\bar{x}_1\bar{x}_2}(t_2,t')\,G^>_{\bar{g}_f g_f}(t',t)\,G^>_{x_2x_1}(t,t_1)\,G^<_{g_i\bar{g}_i}(t_1,t_2) \end{aligned} \tag{6}$$

where $\zeta_{g_i} = 1$ (-1) when state $|g_i\rangle$ is of Fermi (Bose) type, $G^{\gtrless}_{S_1S_2}(t_1,t_2)$ are greater/lesser projections of the Green function (5), $\Pi^{\gtrless}$ are greater/lesser projections of the self-energies due to coupling to radiation field. The Fourier transforms of the latter are[37]

$$\begin{aligned} \Pi^>_{gx,g'x'}(\omega) \equiv -i\Omega_{gx,g'x'}(\omega)\,[1+N(\omega)] \\ \Pi^<_{gx,g'x'}(\omega) \equiv -i\Omega_{gx,g'x'}(\omega)\,N(\omega) \end{aligned} \tag{7}$$

where $\Omega_{gx,g'x'}(\omega) \equiv 2\pi\sum_\alpha V^{(rad)}_{gx,\alpha} V^{(rad)}_{\alpha,g'x'} \delta(\omega-\nu_\alpha)$ and $N(\omega) \equiv \frac{1}{\pi}\frac{\gamma^2}{(\omega-\nu_i)^2+\gamma^2}$ with ν_i being the fre-

quency of the incoming laser radiation, γ - laser bandwidth, and $N(\omega)$ characterizing laser resolution. Note that Eq.(6) is an expression for 'the normal Raman process' as discussed in Refs.[29,30] Note also that it is a time-dependent generalizaton similar to the CT-Raman consideration of Refs.[34,35] At steady-state Eq.(6) becomes $J = \int \frac{d\omega_f}{2\pi} J(\omega_f)$ with

$$J(\omega_f) = -\sum_{\substack{g_i,x_1,x_2,g_f \\ \bar{g}_i,\bar{x}_1\bar{x}_2,\bar{g}_f}} \zeta_{g_i} \int \frac{d\omega_i}{2\pi} \int \frac{dE_i}{2\pi} \int \frac{dE_f}{2\pi} \quad (8)$$

$$2\pi\delta(\omega_i + E_i - \omega_f - E_f)\,\Pi^{<}_{g_i x_1,\bar{g}_i\bar{x}_1}(\omega_i)\,\Pi^{>}_{g_f x_2,\bar{g}_f\bar{x}_2}(\omega_f)$$

$$\int \frac{dE_{\bar{x}}}{2\pi} \int \frac{dE_x}{2\pi} \frac{G^{>}_{\bar{g}_f g_f}(E_f)\,G^{>}_{\bar{x}_1\bar{x}_2}(E_{\bar{x}})\,G^{>}_{x_2x_1}(E_x)\,G^{<}_{g_i\bar{g}_i}(E_i)}{[\omega_i + E_i - E_{\bar{x}} - i\eta][\omega_i + E_i - E_x + i\eta]}$$

where $\eta \to 0^+$ is an infinitesimal real number, $\delta(\ldots)$ is the Dirac delta function. Expression (8) is convenient to use for numerical simulations as described below.

We apply the method introduced above to an OPV3 junction (see Fig. 1a), which was the focus of recent Raman measurements.[19] We chose parameters to be representative of a realistic experimental situation. Following Refs.[60–62] we assume that at low bias the main contribution to conductance comes from neutral (N) and cation (C) states of OPV3, and that $E^e_N - E^e_C - E_F = 0.05$ eV[63,64] (here E^e_N, E^e_C, and E_F are electronic energies of neutral and cation OPV3 species, and the Fermi energy, respectively). The electron escape rates to the contacts, $\Gamma_{L(R)} \equiv 2\pi\sum_{k\in L(R)}|V_{CN,k}|^2\delta(E-\varepsilon_k)$, are taken as 15 meV in agreement with experimental estimate.[65] Molecular vibrations are modeled as harmonic oscillators (normal modes specific for cation and neutral molecule). The dissipation matrix for the vibrations due to coupling to thermal bath is assumed to be diagonal, $\Gamma^B_{\nu^{(m)}\nu^{(m)}+1,\nu^{(m)}\nu^{(m)}+1} \equiv 2\pi\sum_{\beta\in B}|W_{\nu^{(m)}\nu^{(m)}+1,\beta}|^2\delta(\omega-\omega_\beta)$, and the rates are 2.5 meV. The laser field is assumed to be polarized along the principle axis of the OPV3 molecule. The intensity of the field is $\mathscr{E}_i \sim 10^{10}$ V/m, its frequency is $\nu_i = 1.4$ eV, and laser bandwidth $\gamma = 1$ meV. Temperature in the contacts is taken as 100 K. Calculations were preformed on an adjustable energy grid.

Parameters of electronic and vibrational structure of the isolated molecule (ground and excited state electronic energies, normal mode frequencies and electronic transition dipole moments of neutral and cation species) were computed with Density Functional Theory (DFT) and Time Dependent DFT (TDDFT) methodologies.[66,67] For all calculations we use the B3LYP hybrid-functional with a 3-21+G basis set as implemented in the *Gaussian*'09 software package.[68]

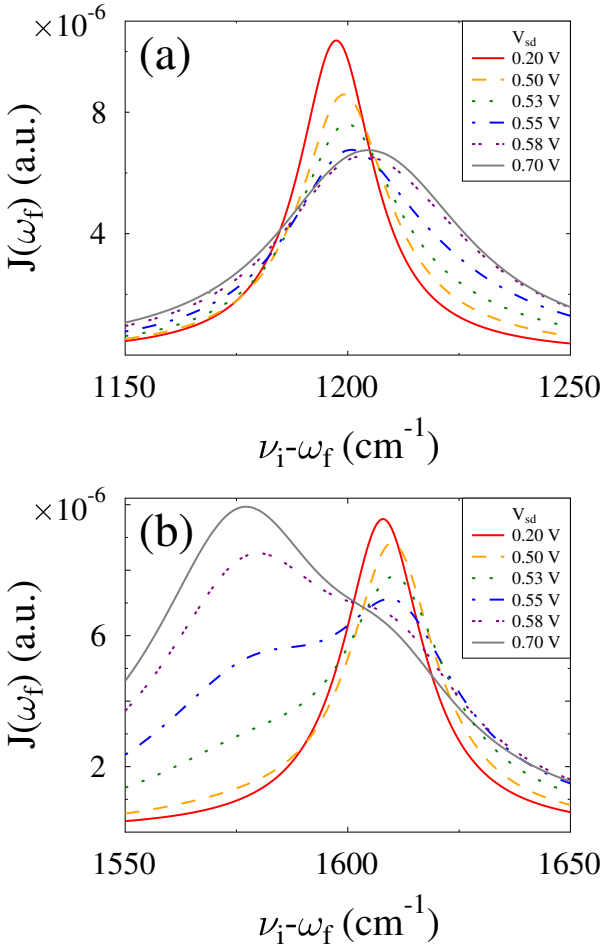

Figure 2: The Stokes peak, Eq.(8), vs. Raman shift for several source-drain biases, V_{sd}. Shown are results for molecular vibrational modes at (a) 1199 and (b) 1608 cm^{-1}. See text for parameters used for simulations.

Figure 2 shows the Stokes shift of two Raman active normal modes. For the neutral OPV3 these modes are at 1199 and 1608 cm^{-1} with displacements schematically shown in Figs. 1b and c. Oxidation of the molecule leads to shift of the modes to 1211 and 1577 cm^{-1}, respectively. Under finite bias both neutral and cation species contribute to the total Raman signal, with the latter contri-

bution becoming more pronounced at higher bias. Correspondingly, the Stokes peak shifts to higher or lower frequencies for the two modes. Note that calculation in Fig. 2a employs $\nu_i = 1.2$ eV as frequency of the laser field. Note also that the shift for the mode at 1608 cm^{-1} (see Fig. 2b) was observed experimentally[16,19] and discussed theoretically within a perturbation theory analysis of electron-vibration coupling.[69] At finite bias charge transfer between the molecule and contacts induces dissipation in the ground states of the neutral and cation species, which leads to broadening of the peaks. We note that the PP-NEGF approach is especially convenient for describing this system since it easily accounts for the different vibrational frequencies of the neutral and cation species while retaining information on mixture of molecular states with those of the contacts. This allows for high accuracy treatment of the electron-vibration coupling in junction which goes far beyond usual considerations within perturbation theory.[37,57]

Dependence of the anti-Stokes peak on bias is shown in Fig. 3a. In addition to the shift of the peak position, as discussed above, heating of the vibration by electric flux results in an increase of the anti-Stokes peak amplitude at higher bias, as is observed in the experiment.[19] It is interesting to note that the shift in the anti-Stokes line is smaller than that of the Stokes peak. While in general there are a number of reasons for such shifts (for example, Stark effect or shift of the line induced by the molecule-contacts hybridization), here we argue that the main contribution comes from renormalization of molecular vibration under oxidation. Thus the shift under bias is defined by relative contributions from neutral molecule and cation to the total Raman signal. In a simplified picture, these contributions to Stokes and anti-Stokes lines are proportional to populations of the ground and excited states of the to species, respectively. Bias induced transfer of electronic population probability from vibronic states of neutral molecule to those of the cation is proportional to the corresponding Franck-Condon factors. The latter are stronger for ground state, which results in more pronounced shift in the Stokes line. We note that different shifts of the Stokes and anti-Stokes lines with bias are consistent with the experimental data (see Figure 3b in Ref.[19]).

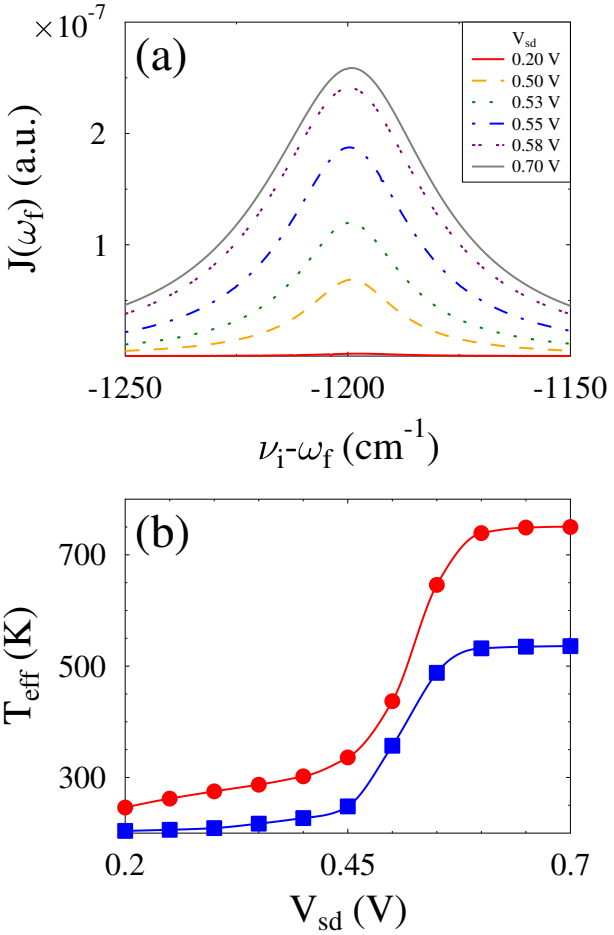

Figure 3: Bias induced vibrational heating. Shown are (a) the anti-Stokes peak, Eq.(8), of molecular vibration at 1199 cm^{-1} vs. Raman shift for several source-drain biases, V_{sd}; (b) Effective temperature vs. applied bias for molecular vibrational modes at 1608 cm^{-1} (squares, blue) and 1199 cm^{-1} (circles, red). See text for parameters used for simulations.

While the temperature of nonequilibrium system is not defined, the notion of "effective temperature" is often utilized in experiments to characterize the extent of bias induced heating in the molecule.[17–19] In particular, effective vibrational temperature, describing extent of vibrational excitation by electron flux, may be estimated from spectroscopic data utilizing ratio of anti-Stokes to Stokes peaks as

$$J(\nu_i + \omega_v)/J(\nu_i - \omega_v) \approx e^{-\hbar\omega_v/k_B T_{eff}} \qquad (9)$$

(here ω_v is frequency of the normal mode of the

neutral molecule). Figure 3b displays result of this estimate. Note that the calculated effective temperature is in agreement with the experimental data (compare with Fig. 3a in Ref.[19]).

In conclusion, we presented a pseudo-particle formulation for Raman spectroscopy in molecular junctions. This framework allows us to describe open non-equilibrium molecular system in the language of many-body states of the isolated molecule. The method treats all intra-molecular interactions exactly, while also keeping the information on hybridization between molecular states and those of the contacts, and on the non-equilibrium electronic population in the molecule. We further applied this methodology to simulate the Raman response of the OPV3 molecular junction under bias, where high quality experimental data recently became available. Parameters of the electronic and vibrational structure of the molecule were obtained from DFT and TDDFT quantum-chemical calculations and from experimental data. Our modeling results demonstrate a shift to lower frequencies and broadening of the Stokes line, reproducing the experimental trends. We argue that such a shift may be caused by the cation contribution to Raman scattering, and that in principle also a shift of the line to higher frequencies may be observable. Our estimate of vibrational heating caused by electric current is also in agreement with experimental data. Thus presented PP-NEGF methodology provides a convenient way to incorporate electronic information obtained for an isolated molecule in equilibrium with convectional quantum-chemical tools to simulate non-equilibrium dynamics of current carrying junctions. We believe that the developed method constitutes an important step towards full *ab initio* calculations of optical response in molecular junctions.

Acknowledgement

We gratefully acknowledge support by the Department of Energy (M.G., Early Career Award, DE-SC0006422) and the Center for Integrated Nanotechnologies (CINT) at Los Alamos National Laboratory (LANL). LANL is operated by Los Alamos National Security, LLC, for the National Nuclear Security Administration of the U.S. Department of Energy under contract DE-AC5206NA25396.

Supporting Information Available

Derivation of Eq. (6) and computational details (OPV3 chemical and electronic structure, and information on normal modes) are provided in the Supporting Information. This material is available free of charge via the Internet at http://pubs.acs.org.

References

(1) Aviram, A.; Ratner, M. A. *Chem. Phys. Lett.* **1974**, *29*, 277–283.

(2) Fleischmann, M.; Hendra, P.; McQuillan, A. *Chem. Phys. Lett.* **1974**, *26*, 163–166.

(3) Jeanmaire, D. L.; Van Duyne, R. P. *J. Electroanal. Chem.* **1977**, *84*, 1–20.

(4) Nie, S.; Emory, S. R. *Science* **1997**, *275*, 1102–1106.

(5) Kneipp, K.; Wang, Y.; Kneipp, H.; Perelman, L. T.; Itzkan, I.; Dasari, R. R.; Feld, M. S. *Phys. Rev. Lett.* **1997**, *78*, 1667–1670.

(6) Qian, X.-M.; Nie, S. M. *Chem. Soc. Rev.* **2008**, *37*, 912–920.

(7) Wustholz, K. L.; Brosseau, C. L.; Casadio, F.; Van Duyne, R. P. *Phys. Chem. Chem. Phys.* **2009**, *11*, 7350–7359.

(8) Sharma, B.; Frontiera, R. R.; Henry, A.-I.; Ringe, E.; Duyne, R. P. V. *Materials Today* **2012**, *15*, 16 – 25.

(9) Moskovits, M. *Phys. Chem. Chem. Phys.* **2013**, *15*, 5301–5311.

(10) Kleinman, S. L.; Frontiera, R. R.; Henry, A.-I.; Dieringer, J. A.; Van Duyne, R. P. *Phys. Chem. Chem. Phys.* **2013**, *15*, 21–36.

(11) Michaels, A. M.; Jiang, J.; Brus, L. *J. Phys. Chem. B* **2000**, *104*, 11965–11971.

(12) Ward, D. R.; Grady, N. K.; Levin, C. S.; Halas, N. J.; Wu, Y.; Nordlander, P.; Natelson, D. *Nano Lett.* **2007**, *7*, 1396–1400.

(13) Banik, M.; Nag, A.; El-Khoury, P. Z.; Rodriguez Perez, A.; Guarrotxena, N.; Bazan, G. C.; Apkarian, V. A. *J. Phys. Chem. C* **2012**, *116*, 10415–10423.

(14) Shamai, T.; Selzer, Y. *Chem. Soc. Rev.* **2011**, *40*, 2293–2305.

(15) Galperin, M.; Nitzan, A. *Phys. Chem. Chem. Phys.* **2012**, *14*, 9421–9438.

(16) Natelson, D.; Li, Y.; Herzog, J. B. *Phys. Chem. Chem. Phys.* **2013**, *15*, 5262–5275.

(17) Ioffe, Z.; Shamai, T.; Ophir, A.; Noy, G.; Yutsis, I.; Kfir, K.; Cheshnovsky, O.; Selzer, Y. *Nature Nanotech.* **2008**, *3*, 727–732.

(18) Ward, D. R.; Halas, N. J.; Ciszek, J. W.; Tour, J. M.; Wu, Y.; Nordlander, P.; Natelson, D. *Nano Lett.* **2008**, *8*, 919–924.

(19) Ward, D. R.; Corley, D. A.; Tour, J. M.; Natelson, D. *Nature Nanotech.* **2011**, *6*, 33–38.

(20) Liu, Z.; Ding, S.-Y.; Chen, Z.-B.; Wang, X.; Tian, J.-H.; Anema, J. R.; Zhou, X.-S.; Wu, D.-Y.; Mao, B.-W.; Xu, X.; Ren, B.; Tian, Z.-Q. *Nat. Commun.* **2011**, *2*, 305.

(21) Jiang, N.; Foley, E. T.; Klingsporn, J. M.; Sonntag, M. D.; Valley, N. A.; Dieringer, J. A.; Seideman, T.; Schatz, G. C.; Hersam, M. C.; Van Duyne, R. P. *Nano Lett.* **2012**, *12*, 5061–5067.

(22) El-Khoury, P. Z.; Hu, D.; Apkarian, V. A.; Hess, W. P. *Nano Lett.* **2013**, *13*, 1858–1861.

(23) Matsuhita, R.; Horikawa, M.; Naitoh, Y.; Nakamura, H.; Kiguchi, M. *J. Phys. Chem. C* **2013**, *117*, 1791–1795.

(24) Banik, M.; El-Khoury, P. Z.; Nag, A.; Rodriguez-Perez, A.; Guarrottxena, N.; Bazan, G. C.; Apkarian, V. A. *ACS Nano* **2012**, *6*, 10343–10354.

(25) Zhang, R.; Zhang, Y.; Dong, Z. C.; Jiang, S.; Zhang, C.; Chen, L. G.; Zhang, L.; Liao, Y.; Aizpurua, J.; Luo, Y.; Yang, J. L.; Hou, J. G. *Nature* **2013**, *498*, 82–86.

(26) Banik, M.; Apkarian, V. A.; Park, T.-H.; Galperin, M. *J. Phys. Chem. Lett.* **2013**, *4*, 88–92.

(27) Konishi, T.; Kiguchi, M.; Takase, M.; Nagasawa, F.; Nabika, H.; Ikeda, K.; Uosaki, K.; Ueno, K.; Misawa, H.; Murakoshi, K. *J. Am. Chem. Soc.* **2013**, *135*, 1009–1014.

(28) Chen, H.; Schatz, G. C.; Ratner, M. A. *Rep. Prog. Phys.* **2012**, *75*, 096402.

(29) Galperin, M.; Ratner, M. A.; Nitzan, A. *Nano Lett.* **2009**, *9*, 758–762.

(30) Galperin, M.; Ratner, M. A.; Nitzan, A. *J. Chem. Phys.* **2009**, *130*, 144109.

(31) Galperin, M.; Nitzan, A. *J. Phys. Chem. Lett.* **2011**, *2*, 2110–2113.

(32) Galperin, M.; Nitzan, A. *Phys. Rev. B* **2011**, *84*, 195325.

(33) Oren, M.; Galperin, M.; Nitzan, A. *Phys. Rev. B* **2012**, *85*, 115435.

(34) Park, T.-H.; Galperin, M. *Europhys. Lett.* **2011**, *95*, 27001.

(35) Park, T.-H.; Galperin, M. *Phys. Rev. B* **2011**, *84*, 075447.

(36) Park, T.-H.; Galperin, M. *Phys. Scr. T* **2012**, *151*, 014038.

(37) White, A. J.; Fainberg, B. D.; Galperin, M. *J. Phys. Chem. Lett.* **2012**, *3*, 2738–2743.

(38) Jensen, L.; Aikens, C. M.; Schatz, G. C. *Chem. Soc. Rev.* **2008**, *37*, 1061–1073.

(39) Dieringer, J. A.; Wustholz, K. L.; Masiello, D. J.; Camden, J. P.; Kleinman, S. L.; Schatz, G. C.; Van Duyne, R. P. *J. Am. Chem. Soc.* **2009**, *131*, 849–854.

(40) Morton, S. M.; Jensen, L. *J. Am. Chem. Soc.* **2009**, *131*, 4090–4098.

(41) Chen, H.; McMahon, J. M.; Ratner, M. A.; Schatz, G. C. *J. Phys. Chem. C* **2010**, *114*, 14384–14392.

(42) Zhao, L.-B.; Huang, R.; Huang, Y.-F.; Wu, D.-Y.; Ren, B.; Tian, Z.-Q. *J. Chem. Phys.* **2011**, *135*, 134707.

(43) Payton, J. L.; Morton, S. M.; Moore, J. E.; Jensen, L. *J. Chem. Phys.* **2012**, *136*, 214103.

(44) Mullin, J.; Schatz, G. C. *J. Phys. Chem. A* **2012**, *116*, 1931–1938.

(45) Zhao, L. L.; Jensen, L.; Schatz, G. C. *Nano Lett.* **2006**, *6*, 1229–1234.

(46) *Spectrochim. Acta A Mol. Biomol. Spectrosc.* **2010**, *75*, 794–798.

(47) Mirjani, F.; Thijssen, J. M.; Ratner, M. A. *J. Phys. Chem. C* **2012**, *116*, 23120–23129.

(48) Leijnse, M.; Wegewijs, M. R. *Phys. Rev. B* **2008**, *78*, 235424.

(49) Schultz, M. G.; von Oppen, F. *Phys. Rev. B* **2009**, *80*, 033302.

(50) Esposito, M.; Galperin, M. *Phys. Rev. B* **2009**, *79*, 205303.

(51) Esposito, M.; Galperin, M. *J. Phys. Chem. C* **2010**, *114*, 20362–20369.

(52) A more detailed discussion of advantages of the PP-NEGF formulation for Raman scattering in junctions is given in the Supporting Information. .

(53) Ruhoff, P. T. *Chem. Phys.* **1994**, *186*, 355–374.

(54) Ruhoff, P. T.; Ratner, M. A. *Int. J. Quant. Chem.* **2000**, *77*, 383–392.

(55) Eckstein, M.; Werner, P. *Phys. Rev. B* **2010**, *82*, 115115.

(56) Oh, J. H.; Ahn, D.; Bubanja, V. *Phys. Rev. B* **2011**, *83*, 205302.

(57) White, A. J.; Galperin, M. *Phys. Chem. Chem. Phys.* **2012**, *14*, 13809–13819.

(58) Marbach, J.; Bronold, F. X.; Fehske, H. *Phys. Rev. B* **2012**, *86*, 115417.

(59) In our approach we extend ideas of atomic limit formulations to nonequilibtium regime, where the starting point of treatment is an isolated system, and coupling between the system and baths is taken into account within a perturbation theory. Thus ground and excited states used in our method are many-body states of the isolated molecule. .

(60) Crljen, Ž.; Grigoriev, A.; Wendin, G.; Stokbro, K. *Phys. Rev. B* **2005**, *71*, 165316.

(61) Stokbro, K. *J. Phys.: Condens. Matter* **2008**, *20*, 064216.

(62) Bilić, A.; Crljen, Ž.; Gumhalter, B.; Gale, J. D.; Rungger, I.; Sanvito, S. *Phys. Rev. B* **2010**, *81*, 155101.

(63) Hybertsen, M. S.; Venkataraman, L.; Klare, J. E.; Whalley, A. C.; Steigerwald, M. L.; Nuckolls, C. *Journal of Physics: Condensed Matter* **2008**, *20*, 374115.

(64) Das, B. *AIP Conference Proceedings* **2011**, *1349*, 951–952.

(65) Poot, M.; Osorio, E.; O'Neill, K.; Thijssen, J. M.; Vanmaekelbergh, D.; Walree, C. A. v.; Jenneskens, L. W.; van der Zant, H. S. J. *Nano Lett.* **2006**, *6*, 1031–1035.

(66) Parr, R. G.; Yang, W. *Density-Functional Theory of Atoms and Molecules*; Oxford University Press, 1989.

(67) Ullrich, C. A. *Time-Dependent Density-Functional Theory*; Oxford University Press, 2012.

(68) Frisch, M. J. et al. Gaussian 09 Revision D.01. Gaussian Inc. Wallingford CT 2009.

(69) Kaasbjerg, K.; Novotný, T.; Nitzan, A. *Phys. Rev. B* **2013**, *88*, 201405.